J Nanostruct 15(4): 1661-1670, Autumn 2025

RESEARCH PAPER

Cytotoxicity of Green and Ecofriendly Synthesized Magnesium Oxide Nanoparticles on LS-174T Colorectal Adenocarcinoma Cell Line

Abothur Almohana [1], Khalida Kadhim A. Al-Kelaby [2], Che Azurahanim Che Abdullah [3], Syafinaz Amin-Nordin [4], Rosnah Binti Nawang [5]*

[1] Faculty of Medicine, Jabir Ibn Hayyan University of Medical and Pharmaceutical Sciences, Najaf, Iraq

[2] Department of Clinical and Laboratory Sciences, College of Pharmacy, University of Kufa, Iraq

[3] Department of Physics, Faculty of Science, University Putra Malaysia, Serdang 43400, Selangor, Malaysia

[4] Department of Medical Microbiology, Faculty of Medicine and Health Sciences, Universiti Putra Malaysia, Malaysia

[5] Institute of Nanoscience and Nanotechnology, University Putra Malaysia, Serdang 43400, Selangor, Malaysia

ARTICLE INFO

Article History:
Received 05 June 2025
Accepted 14 August 2025
Published 01 October 2025

Keywords:
Cell culture
Green synthesis
LS-174T colorectal adenocarcinoma
MTT Assay
MgO-NPs

ABSTRACT

Scientists are using nanotechnology in a variety of sectors, including dentistry, oncology, illness diagnosis and treatment, and the cosmetics industry, as they become more aware of the benefits of nano pharmaceuticals. This study uses the Thiazolyl blue tetrazolium bromide (MTT) cytotoxicity assay and the standard anticancer chemotherapeutic drug 5-fluorouracil (5FU) to examine the toxicological effects of magnesium oxide nanoparticles (MgO-NPs) at various concentrations (1,10,100,500, and 1000 µg/mL) on the LS-174T colorectal adenocarcinoma cell line. Zinc nitrate salts and aqueous extraction of dill extract were used to create magnesium oxide nanoparticles. Since green extraction processes use non-toxic chemicals, creating nanoparticles in environmentally benign ways is particularly interesting. One emerging area in nanotechnology is green synthesis techniques, especially those that use biological systems such as plant extracts. X-ray diffraction (XRD), scanning electron microscopy (SEM), and Fourier-transform infrared spectroscopy (FT-IR) were among the methods used to characterize the synthesized MgO-NPs. This investigation demonstrated that MgO-NPs had positive therapeutic selectivity index efficacy in cell killing and inhibition (SI=2.98; IC50 = 51.26 µg/mL). It also emphasized size-dependent effects, whereby the smaller size and possible chemical lability of nanoparticles may boost cell uptake and interaction, hence resulting in increased cytotoxicity. These results have encouraging ramifications for MgO-NPs' therapeutic uses in cancer treatment.

How to cite this article
Almohana A., Al-Kelaby K., Abdullah C., Amin-Nordin S., Nawang R. Cytotoxicity of Green and Ecofriendly Synthesized Magnesium Oxide Nanoparticles on LS-174T Colorectal Adenocarcinoma Cell Line. J Nanostruct, 2025; 15(4):1661-1670. DOI: 10.22052/JNS.2025.04.014

INTRODUCTION

In 2020, cancer was responsible for nearly 10 million fatalities, which is equivalent to nearly one in six deaths worldwide. Breast, lung, colon, rectum, and prostate malignancies are the most prevalent types of cancer [1]. Numerous researchers have endeavored to identify an effective solution for cytotoxic medications that

* Corresponding Author Email: abothur.almohana@jmu.edu.my

can be efficiently delivered to tumor tissues using nanoparticles, which are reliant on complex pharmacological concepts. Nanomedicine can also be used to develop a variety of pharmaceuticals at the cancer site, which exhibits superior cytotoxic effects. Nanomedicine also offers a targeted chemotherapeutic approach that is still in the process of development. This field facilitates the targeted distribution of drugs to the cancer site by increasing the permeability of the blood vessels at the tumor sites. The scope of anticancer nanomedicine [2].

Nano biotechnology is the fusion of the biotechnology and nanotechnology fields. Traditional biotechnological methods are enhanced by the development of nano-based approaches, which are designed to address their shortcomings, including the adverse effects of conventional therapies. Nano biotechnology has significantly improved the efficacy of a variety of techniques, such as drug delivery, water and soil remediation, and enzymatic processes, according to numerous studies [3].

The metal oxide nanoparticles have been commonly utilized in biology-based applications like tissue and cell engineering, therapeutic, diagnostic, and drug delivery purposes. MgO is a non-toxic elemental metal oxide that has been used as a modifying agent, and catalyst, in superconductors and elsewhere in industry and medicine. Usually, MgO-NPs are fabricated through different methods such as sol-gel, flame spray pyrolysis, aqueous wet chemical, laser vaporization, hydrothermal, synthesis, combustion aerosol, as well as surfactant approaches [4]. The green synthesis approach has garnered significant attention as a sustainable, reliable, and environmentally friendly method for synthesizing various nanomaterials. Notably, plant-based nanomaterials are a valuable source of numerous biologically active metabolites such as ascorbic acid, flavonoids, alkaloids, and terpenoids [5]. Plant extracts, such as those from dill seeds (*Anethum graveolens*); contain various volatile components, with carvone being the main constituent. Additionally, they contain alpha-phellandrene, dill ether, flavonoids, myristicin, limonene, eugenol, anethole, coumarin, triterpenes, phenolic acids, and umbelliferone. The Anethum graveolens plant exhibits distinct pharmacological effects, including anticancer, antiulcer, anti-inflammatory, antioxidant, and antimicrobial properties [6]. There are studies in 2023 that say potential biological applications of biosynthesized MgO-NPs as a therapeutic catalyst, anti-cancer drug, anti-diabetic agent, anti-microbial agent, electrochemical biosensor, curing agent, paints, and superconductors and also as an anti-microbial agent that has led to systemic resistance. in plants against bacterial wilt disease caused by phytopathogenic bacteria [7]. The activity of magnesium ions in enhancing angiogenesis has been previously studied to understand the importance of osteogenic and angiogenic coupling for complete bone regeneration [8].

MATERIALS AND METHODS

Preparation of Extract

Plant materials have been used in the green synthesis of nanoparticles, and researchers have extensively studied locally available plants in large quantities. These studies highlight the full potential of utilizing local plants; however, achieving large-scale global production remains challenging. Fresh dill leaves were sourced from local markets in Kuala Lumpur in January 2024. After washing the leaves three times with distilled water, they were completely dried in the shade and then finely powdered using a laboratory grinder [9].

The procedure was carried out as follows: 100 ml of deionized water was added to a conical flask, followed by 10 grams of dill plant material. The mixture was stirred using a magnetic stirrer for 90 minutes at a temperature of 60°C. After stirring, white filter paper was used to separate the residue, and the supernatant was retained. The supernatant was stored at 4°C. The extracted solution was later refrigerated at 4°C.

Preparation of Magnesium Oxide Nanoparticles

1.48 grams of Magnesium nitrate were dissolved in deionized water, followed by the gradual addition of the dill extract. Subsequently, a small amount of sodium hydroxide solution with a 0.1 g/mL concentration was added until the pH reached 11. The mixture was placed on a magnetic stirrer at a temperature of 70°C, rotating at 191 rpm for two hours and twenty minutes until a color change was observed. The dill extract acts as a reducing agent for the Magnesium salt compounds and stabilizes the MgO-NPs during synthesis. The solution was centrifuged at 4000 rpm for 15 minutes. Plant-based methods for nanoparticle synthesis offer a green, biocompatible, cost-

effective, environmentally friendly, simple, and easily scalable approach for the commercial production of nanoparticles.

X-ray diffraction (XRD)

The properties of the nano powder were confirmed using a Smart Lab Rigaku-Japan X-ray diffraction device. That analysis was conducted at the Institute of Nanoscience and Nanotechnology, Universiti Putra Malaysia.

Scanning Electron Microscopy (SEM)

The analysis was conducted at the Institute of Biosciences at Putra University, underscoring the extensive use of SEM in advanced research settings.

Fourier Transform Infrared (FTIR)

FTIR is a technique used to obtain the infrared spectrum of absorption, emission, photoconductivity, or Raman scattering of a solid or liquid [10]. This analysis was conducted at the Faculty of Science, Department of Chemistry, and University of Malaya (UM) in Malaysia.

Cytotoxicity assay

Using the MTT assay, the anticancer activity of MgO-NPs was evaluated in the Department of Clinical and Laboratory Sciences, Faculty of Pharmacy, University of Kufa, against the LS-174T colorectal adenocarcinoma cell line (LS-174T (ATCC® CL188™) (Organism: Homo sapiens, human, Colon, Dukes' type B, colorectal adenocarcinoma, American Type Culture Collection) in comparison to 5-fluorouracil (5-FU). In 96-well plates, the cell line was plated at a density of l04 cells/ml. After being incubated for 48 hours at 37°C, the LS-174T monolayer was confluent. The MgO-NPs and 5-FU compounds (1, 10, 100, 500, and 1000 µg/ml) were added in triplicate for each concentration, with a final volume of 100 µl, with the exception of the control cells, which received media alone treatment. After being incubated for 48 hours at 37°C in 5% CO2, cell monolayers were washed with PBS solution three times to remove any remaining residues of traditional anticancer drugs or colorimetric substances that might have affected the MTT readings. All wells of treated , untreated, and blank wells were received a volume of 20 µl of MTT reagent (bio WORLD, USA) after 100 µl of maintenance media, and incubated for 3 hours at 37°C and 5% carbon dioxide. LS-174T created formazan molecules by an enzymatic mitochondrial process; dead cells, on the other hand, were unable to produce formazan particles because of abnormalities in their mitochondrial organelles. To dissolve the formazan, dimethylsulfoxide (DMSO) was applied 1:1 in isopropanol to every well—including the blank wells. The absorbance was measured at 490 *nm* with a reference wavelength of *630 nm* by an ELISA reader (Model wave xs2, BioTek, USA)... The 50% cytotoxic concentration (IC50) causing 50% of visible cellular morphological changes in cells with respect to cell control was calculated [11,12].

Statistical analysis

Statistical analyses were performed using SPSS 21.0 Inc. for windows. Inc. Data were expressed as mean ± SEM unless otherwise stated by ANOVA test. In all tests, R^2 was computed using the Pearson Correlation Coefficient. $P<0.05$ was considered to be statistically significant. Halve inhibitory concentration was fitted by blotting of inhibition percentage versus log of concentration of any compound used. Growth inhibition % was calculated using formula: % of growth Inhibition =[(A−A1)/A]×100; Where A=absorbance of untreated samples, A1= absorbance of the treated test/standard. While the 50% of maximum inhibition (=Y in the formula of IC50 calculation) was calculated according to the following equation: 50% of maximum inhibition=Max % of growth Inhibition - 50% × (Max % of growth Inhibition - min % of growth Inhibition).

RESULTS AND DISCUSSION

XRD measurements

X-ray diffraction (XRD) analysis was performed to assess the crystal structure, phase purity, and particle size of the synthesized MgO-NPs. Fig. 1 illustrates the XRD pattern, which displays several peaks corresponding to the (111), (200), (220), (311), and (222) reflection planes. These peaks indicate that MgO-NPs has a cubic crystalline structure and aligns with the pure phase of periclase MgO [13]. Importantly, no additional peaks were present, confirming that the product is free from impurities and is indeed crystalline. Additionally, the peaks are characterized by high intensity and narrow widths, which imply that the MgO-NPs exhibits excellent crystallinity. The particle size of the synthesized MgO-NPs was determined using the Debye-Scherrer equation:

$$D=K\lambda/\beta\cos\theta \quad (1)$$

In this formula, K represents a shape factor set at 0.9, λ is the wavelength, θ is the angle β corresponding to the full width at half maximum height of the diffraction peak for the (200) reflection plane, and D denotes the crystallite size. The average crystallite size of the synthesized MgO-NPs was found to be 20 nm, respectively. Overall, the XRD analysis confirmed that the material consists solely of cubic MgO-NPs, with a lattice constant (a) measured at 0.435 nm. The 2θ positions of MgO powder are consistent with JCPDS card no: 75–0447 [14], which is evident in the cubic crystalline structure. Consequently, the particle of MgO-NPs that was mediated by green light exhibited a crystalline structure that was exceedingly pure, devoid of any other diffraction peaks. The most basic elements include the size, shape, chemical composition, and surface modification of NPs. Additionally, the interaction between NPs and proteins can also influence the biological effects of NPs. Smaller particles demonstrate larger surface areas, which facilitates intricate interactions with cellular components such as carbohydrates, fatty acids, proteins, and nucleic acids. Consequently, the size of NPs emerged as a significant factor. These findings indicate that the cytotoxic efficacy of NPs may be influenced by their particle size [15].

Scanning Electron Microscopy (SEM)

The morphology of the MgO-NPs was examined using scanning electron microscopy (SEM). As depicted in Fig. 2 (A-C), the resulting material comprises uniform nanocrystals exhibiting a spherical shape. The image clearly indicates that most of the particles are agglomerated and display rough surfaces. SEM technique provides a straightforward means of assessing the particle size of nanomaterials. Fig. 2B and C present SEM images of the synthesized MgO-NPs in higher magnification, with an average particle size estimated at 20 nm. These findings are consistent with the XRD results, where particle size was calculated using the Scherrer formula. The formation of overlapping irregular blade-type particles was observed in the SEM images of the MgO-NPs, suggesting a certain inclination towards aggregation, agglomeration, and an abrasive surface, which can be attributed to interparticle interactions among smaller particles due to Van der Waals, electrostatic, or magnetic forces. These results were in agreement with the findings of other recent study [16].

Fourier Transform Infrared (FTIR)

Infrared spectroscopy analysis identifies the functional groups, such as phenolic groups and metal ion bonding. Fig. 3 displays the infrared spectra of magnesium oxide nanostructures prepared using green chemistry. The absorption peaks observed at 3467.40, 3662.86, 3789.20, and 3019.26cm^{-1} correspond to the hydroxyl stretching vibration of the O-H bond in alcohols and phenols. The peaks at 2799.44 and 2118.85 cm^{-1} indicate the presence of C-H stretching bonds in aromatic aldehydes. The peak absorbed at 1,796 cm^{-1} corresponds to the C=O stretching vibration of carbonyl groups, while the peak at 1,048 cm^{-1} corresponds to the C-O stretching vibration, suggesting the presence of saturated primary alcohols [17]. The peaks absorbed in the range of 1404–1422 cm^{-1} correspond to the αCH2 bending vibration, indicating the presence of aromatic

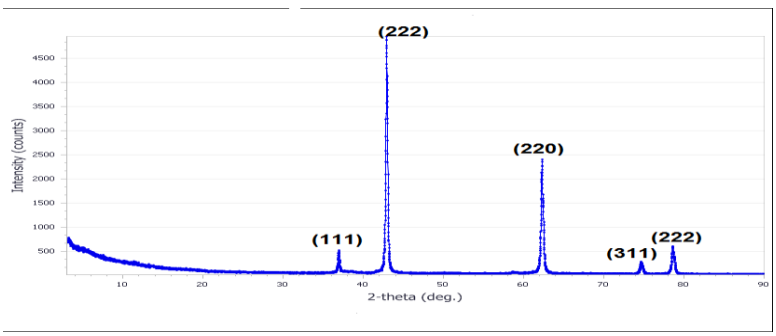

Fig. 1. XRD pattern of the synthesized MgO-NPs.

tertiary amine groups, aldehydes, and ketones. The absorption peaks at 1137 and 1123 cm^{-1} suggest the presence of carboxylic acids, esters, and alcohols. The absorption peaks in the range of 667–557 cm^{-1} and 870–865 cm^{-1} correspond to the Mg-O stretching vibration, confirming the presence of MgO-NPs [18].

Cytotoxicity assay

Results showed significant anticancer activity of MgO-NPs against the LS-174T colorectal cancer cell line as compared with untreated cells (P<0.000). The IC50 value was equal to 51.26 µg / ml, with positive correlation coefficient value (0.914), while showing IC50 of 152.78 µg / ml, on VERO cells, with significant statistically differences (p<0.05) and positive correlation coefficient (0.6867), as shown in Fig. 4 and 6 respectively. The standard anticancer drug (5FU) also showed IC50 of 7.81 µg/ml, and correlation coefficient of 0.7088 on cancer cells, Fig. 5, while showing IC50 of 91.7 µg/ml on VERO cells as shown in Fig. 7. These results showed positive therapeutic selectivity index (2.98) for MgO-NPs, while 11.74 for 5FU. The anticancer values of MgO-NPs and 5 fluorouracil compounds presented by mean± SEM and GI% values of both LS-174T colorectal cancer and VERO cells were shown in Tables 1 and 2 respectively. While separated growth inhibition curves were presented in Figs. 4-7.

Positive Pearson correlation coefficient value (0.914) between MgO-NPs dose and response indicated dose dependency of cell cytotoxicity after treatment with different concentrations of green synthesized MgO-NPs. These results were consistent with the fact that the biogenic MgO

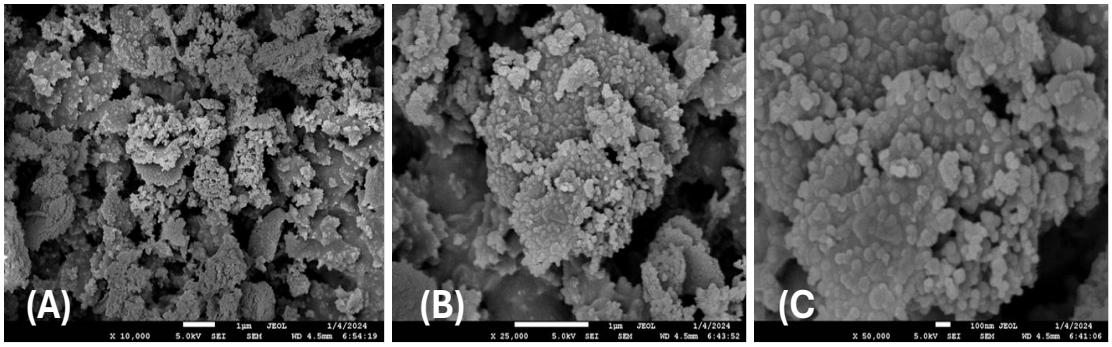

Fig. 2. SEM images of MgO-NPs prepared using green chemistry in different magnifications.

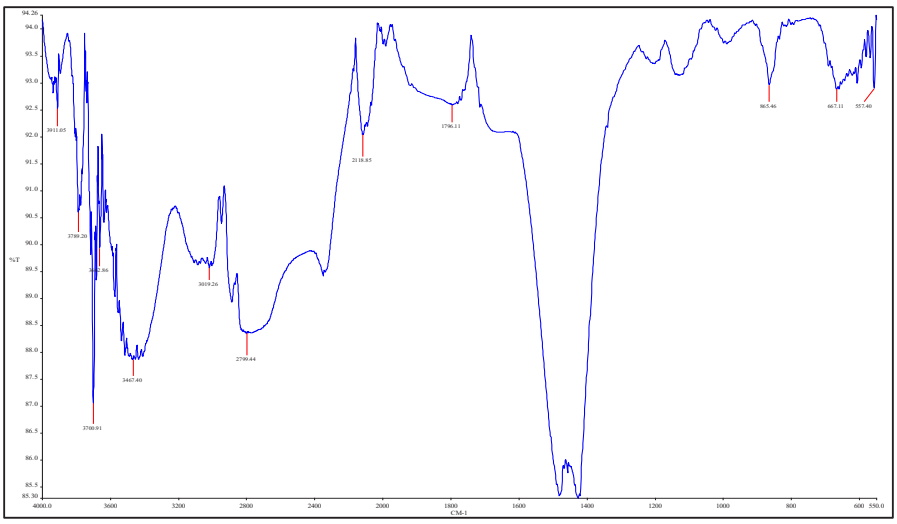
Fig. 3. FTIR Spectra of MgO-NPs.

NPs exhibited increased cytotoxicity, induced apoptosis, enhanced formation of ROS, promoted cell adhesion and inhibited cellular migration in a dose-dependent manner [19].

Results showed that green synthesized MgO-NPs may have the anticancer potency against LS-174T colorectal adenocarcinoma cell lines, since revealed positive therapeutic selectivity index (2.98) for MgO-NPs, that exhibit a high degree of selectivity and exhibit a highly potent activity at lower concentrations. Values of IC50, R^2 and SI index of MgO-NPs and 5-FU on both VERO or LS-174T cells were presented in Table 3. Growth (nested) inhibition curves of LS-174T and VERO cells after 48 hrs. of incubation with different concentration of MgO-NPs.or 5-Flourouracil were also presented in Fig. 8.

The following formula was used to calculate the selectivity index (SI), which represents the cytotoxic selectivity of MgO-NPs against cancer cells in comparison to normal cells:

$$\text{Selectivity Index} = \frac{\text{IC50 on normal cells}}{\text{IC50 on malignant cells}}$$

High selectivity was defined as SI values that exceeding 2 [19,20].

Over the past few decades, chemotherapeutic agents/pharmaceuticals have been the primary treatment option for advanced-stage malignancies that cannot be treated with surgery and/or radiation therapy for specific reasons. The development of cancer cells can be halted or killed by anti-cancer compounds that are derived from natural sources or their synthetic chemical analogues [21-23]. It is important to note that a variety of alternative

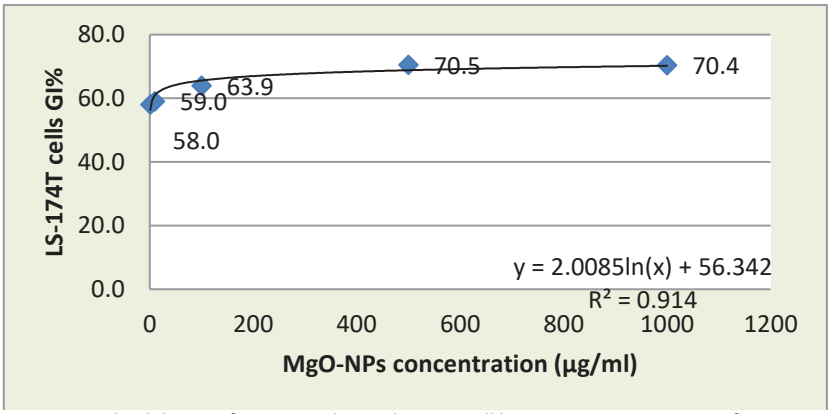

Fig. 4. Growth inhibition of LS-174T colorectal cancer cell line versus concentration of MgO-NPs.

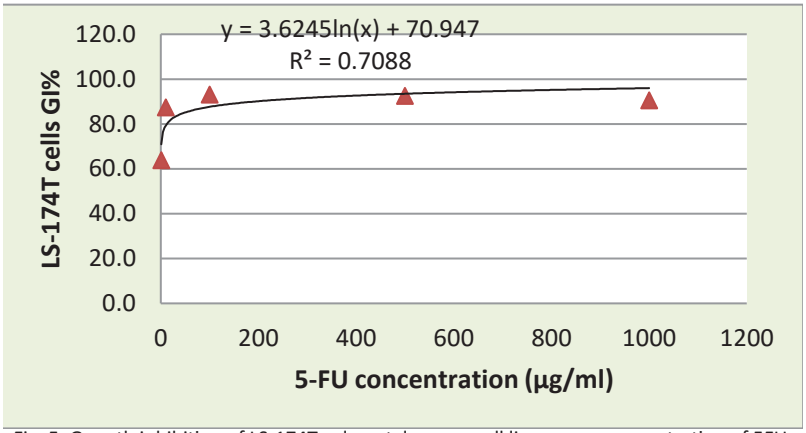

Fig. 5. Growth inhibition of LS-174T colorectal cancer cell line versus concentration of 5FU.

methods are being developed to treat cancer cells [24,25]. Conventional chemotherapy's primary disadvantage is its adverse effects on the body, as it fails to deliver selective and specific action to the cancer cells. Consequently, the damage extends to the surrounding normal healthy tissues or rapidly divides healthy cells, such as those in the bone marrow, gastrointestinal tract, and hair follicles, resulting in issues such as cardiac, hepatic, pulmonary, gastrointestinal, and renal toxicities [26].

While 5FU exhibits antineoplastic activity by inhibiting the thymidylate synthetase (TS), the conversion of deoxyuridylic acid to thymidylic acid, and the incorporation/insertion of its metabolites into RNA and DNA, it is widely used in the treatment of colorectal cancer [26-28]. However, it has numerous adverse effects; topical application is linked to an irritant dermatitis, promotion of vacuolization and decrease of intestinal villi, infiltration of inflammatory cells, other indications of cryptic necrosis, decrease in villus/crypt ratio, and loss of cell architecture [29,30]. The adverse effects of parenteral administration are more severe and include cutaneous reactions, gastrointestinal toxicity, and bone marrow suppression with clinically significant value. The two proposed mechanisms by which doxorubicin acts in the cancer cell are as follows: (i) intercalation into DNA strands and destruction of topoisomerase II-mediated DNA repair (ii) generation of free radicals and subsequent injury

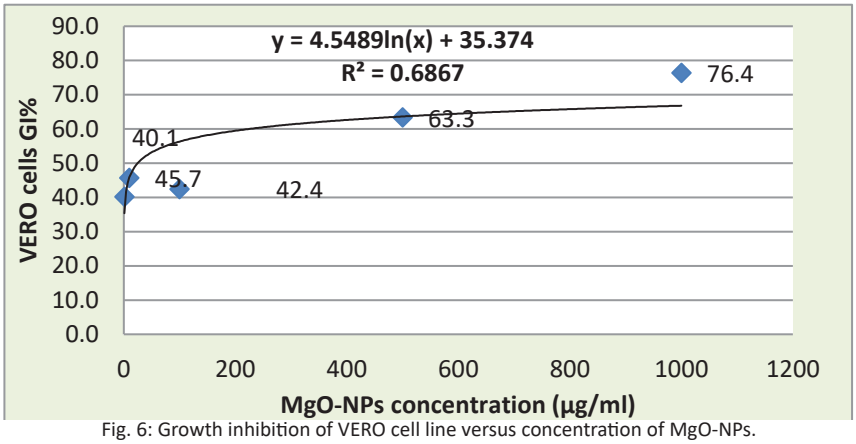

Fig. 6: Growth inhibition of VERO cell line versus concentration of MgO-NPs.

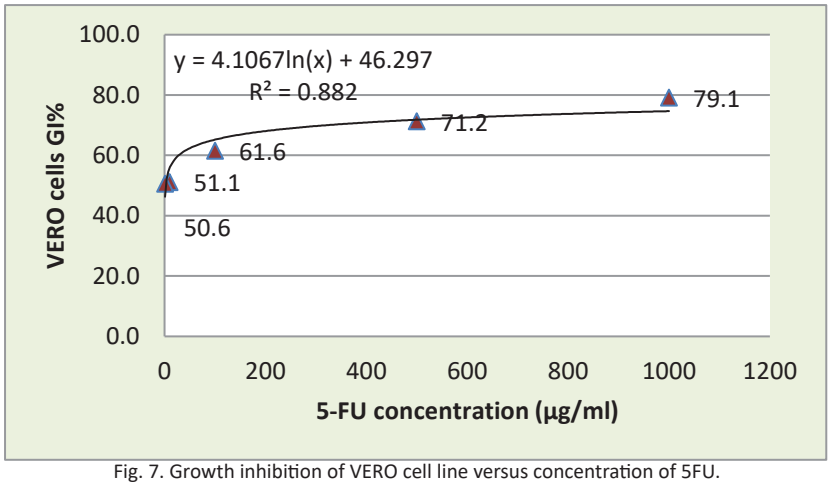

Fig. 7. Growth inhibition of VERO cell line versus concentration of 5FU.

to cellular membranes, nucleic acids (DNA), and proteins [31].

The assay of MTT tetrazolium reduction was the first cell viability assay developed for the evaluation and measurement of any therapeutic agent potency. This assay is regarded as valuable, suitable for multivariate screening and provides accurate and reliable quantification of viability [32]. The MTT assay for cellular metabolic activity is nearly universal in cell toxicity research; however, it is frequently applied and interpreted incorrectly. The applicability and limitations of the MTT assay in representing treatment toxicity, cell viability, and metabolic activity were examined

Table 1. Cytotoxic activity of MgO-NPs on LS-174T and VERO cells presented by Mean±

MgO-NPs	LS-174T cells		VERO cells	
(Dose(µg/ml)	Mean ± SEM	GI%	Mean ± SEM	GI%
0.000	0.732±0.046	0	0.074±0.043	0
1	0.109±0.002	58.0	0.078±0.045	40.1
10	0.102±0. 003	59.0	0.093±0.054	45.7
100	0.066±0.002	63.9	0.159±0.092	42.4
500	0.018±0.014	70.5	0.086±0.049	63.3
1000	0.0187±0.017	70.4	0.065±0.037	76.4

GI%= growth inhibition %; SEM: Standard error of mean; IC50: inhibitory concentration of 50% of cell viability

Table 2. Cytotoxic activity of 5-Flourouracil on LS-174T and VERO cells presented by Mean± SEM and GI% values.

5-FU	LS-174T cells		VERO cells	
(Dose (µg/ml)	Mean ± SEM	GI%	Mean ± SEM	GI%
0.000	0.414± 0.002	0	0.131±0.021	0
1	0.149± 0.0493	63.8	0.065±0.009	50.6
10	0.0517± 0.001	87.4	0.064±0.006	51.1
100	0.029± 0.001	93.0	0.050±0.0147	61.6
500	0.031± 0.000	92.5	0.038±0.009	71.2
1000	0.0387± 0.003	90.6	0.027±0.004	79.1

GI%.; GI%= growth inhibition %; SEM: Standard error of mean; IC50: inhibitory concentration of 50% of cell viability

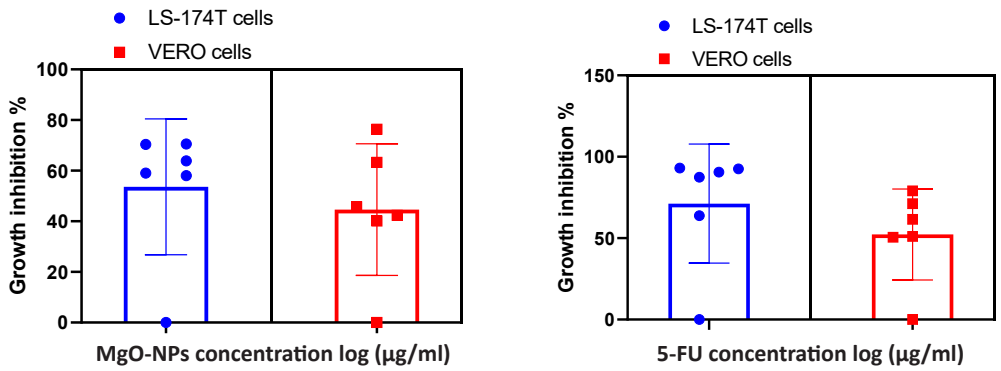

Fig. 8. Growth inhibition of LS-174T and VERO cells after 48 hrs. of incubation with different concentration of MgO-NPs. (A) and 5-Flourouracil (B), plotted by graph pad prism 8.0.2.(263).

Table 3. Cytotoxicity of MgO-NPs and 5-FU presented by IC50 and R^2 value and SI values.

IC50 ,R2 and SI	MgO-NPs		5-FU	
	LS-174T cells	VERO cells	LS-174T cells	VERO cells
IC50 (µg/ml)	51.26	152.78	7.81	91.7
R^2	0.914	0.6867	0.7088	0.882
SI	2.98		11.74	

MgO-NPs= MgO nanoparticles; 5FU=5-Flourouracil; IC50= Half maximal inhibitory concentration; R2 = correlation coefficient o concentration log Vs growth inhibition %.

[33]. Cancer is an abnormal condition in which cells undergo uncontrolled proliferation and produce aggressive malignancies, resulting in millions of fatalities annually. Our comprehension of the disease is expanding as a result of the new understanding of the molecular mechanism(s) of disease progression, which has resulted in the development of numerous new therapeutic regimes and their subsequent trials [34].

MgO-NPs enhanced ultrasound-induced lipid peroxidation in the liposomal membrane. The toxicity of MgO NPs is attributed to the generation of reactive oxygen species, which further results in the induction of apoptosis in cancer cells [35]. A significant contributor to the observed cytotoxicity was identified as the disturbance of intracellular calcium (Ca^{2+}). Despite Ca^{2+} being a pivotal signaling molecule involved in metabolic regulation, its elevated levels were found to induce acute toxicity on cellular mitochondria [36].

CONCLUSION

Results showed that green synthesized MgO-NPs may have the anticancer potency against LS-174T colorectal adenocarcinoma cell lines. These nanoparticles exhibit a high degree of selectivity and exhibit a highly potent activity at lower concentrations. Additional research is required to determine the mechanism of growth suppression and to assess the efficacy of the extract in animal models.

ACKNOWLEDGEMENT

I would like to extend my gratitude and appreciation to the Iraqi Ministry of Higher Education and Scientific Research for their financial support, as well as to Putra University Malaysia.

CONFLICT OF INTEREST

The authors declare that there is no conflict of interest regarding the publication of this manuscript.

REFERENCE

1. Papachristodoulou A, Abate-Shen C. Precision intervention for prostate cancer: Re-evaluating who is at risk. Cancer Lett. 2022;538:215709.
2. Hong L, Li W, Li Y, Yin S. Nanoparticle-based drug delivery systems targeting cancer cell surfaces. RSC Advances. 2023;13(31):21365-21382.
3. Nejati M, Rostami M, Mirzaei H, Rahimi-Nasrabadi M, Vosoughifar M, Nasab AS, et al. Green methods for the preparation of MgO nanomaterials and their drug delivery, anti-cancer and anti-bacterial potentials: A review. Inorg Chem Commun. 2022;136:109107.
4. Shahcheraghi N, Golchin H, Sadri Z, Tabari Y, Borhanifar F, Makani S. Nano-biotechnology, an applicable approach for sustainable future. 3 Biotech. 2022;12(3).
5. Younis IY, El-Hawary SS, Eldahshan OA, Abdel-Aziz MM, Ali ZY. Green synthesis of magnesium nanoparticles mediated from Rosa floribunda charisma extract and its antioxidant, antiaging and antibiofilm activities. Sci Rep. 2021;11(1).
6. Belurkar R. Synthesis and Characterization of Lanthanum Nanoparticles by Anethum Graveolens (Dill) Leaf Extract. Oriental Journal Of Chemistry. 2021;37(5):1205-1209.
7. El-Moslamy SH. Bioprocessing strategies for cost-effective large-scale biogenic synthesis of nano-MgO from endophytic Streptomyces coelicolor strain E72 as an anti-multidrug-resistant pathogens agent. Sci Rep. 2018;8(1).
8. Ravoor J, Amirthalingam S, Mohan T, Rangasamy J. Antibacterial, anti-biofilm and angiogenic calcium sulfate-nano MgO composite bone void fillers for inhibiting Staphylococcus aureus infections. Colloid and Interface Science Communications. 2020;39:100332.
9. Kalangi SK, Dayakar A, Gangappa D, Sathyavathi R, Maurya RS, Narayana Rao D. Biocompatible silver nanoparticles reduced from Anethum graveolens leaf extract augments the antileishmanial efficacy of miltefosine. Exp Parasitol. 2016;170:184-192.
10. Marcott C, Padalkar M, Pleshko N. 3.23 Infrared and Raman Microscopy and Imaging of Biomaterials at the Micro and Nano Scale ☆. Comprehensive Biomaterials II: Elsevier; 2017. p. 498-518. http://dx.doi.org/10.1016/b978-0-12-803581-8.10183-3
11. Cytotoxicity and modulation of synthesized nitrochalcone derivative on rhabdomyosarcoma cell line. Journal of cellular cancer. 2016;8(1):41-51.
12. Bahuguna A, Khan I, Bajpai VK, Kang SC. MTT assay to evaluate the cytotoxic potential of a drug. Bangladesh Journal of Pharmacology. 2017;12(2).

13. Diachenko OV, Opanasuyk AS, Kurbatov DI, Patel SS, Desai RR, Lakshminarayana D, et al. Structure and Substructure Properties of Magnesium Oxide Thin Films. Invertis Journal of Science & Technology. 2016;9(2):72.
14. Khan AU, Khan M, Khan AA, Parveen A, Ansari S, Alam M. Effect of Phyto-Assisted Synthesis of Magnesium Oxide Nanoparticles (MgO-NPs) on Bacteria and the Root-Knot Nematode. Bioinorg Chem Appl. 2022;2022(1).
15. Xuan Y, Zhang W, Zhu X, Zhang S. An updated overview of some factors that influence the biological effects of nanoparticles. Frontiers in Bioengineering and Biotechnology. 2023;11.
16. Balaba N, Primo JdO, Sotiles AR, Jaerger S, Horsth DFL, Bittencourt C, et al. Synthesis of Periclase Phase (MgO) from Colloidal Cassava Starch Suspension, Dual Application: Cr(III) Removal and Pigment Reuse. Physchem. 2024;4(1):61-77.
17. Liu J, Chen F, Yang W, Guo J, Xu G, Jia F, et al. Excess soluble alkalis to prepare highly efficient MgO with relative low surface oxygen content applied in DMC synthesis. Sci Rep. 2021;11(1).
18. Yesiltas M, Glotch TD, Sava B. Nano-FTIR spectroscopic identification of prebiotic carbonyl compounds in Dominion Range 08006 carbonaceous chondrite. Sci Rep. 2021;11(1).
19. Rashidi M, Seghatoleslam A, Namavari M, Amiri A, Fahmidehkar MA, Ramezani A, et al. Selective Cytotoxicity and Apoptosis-Induction of Cyrtopodion scabrum Extract Against Digestive Cancer Cell Lines. International Journal of Cancer Management. 2017;10(5).
20. Machana S, Weerapreeyakul N, Barusrux S, Nonpunya A, Sripanidkulchai B, Thitimetharoch T. Cytotoxic and apoptotic effects of six herbal plants against the human hepatocarcinoma (HepG2) cell line. Chin Med. 2011;6(1).
21. Lichota A, Gwozdzinski K. Anticancer Activity of Natural Compounds from Plant and Marine Environment. Int J Mol Sci. 2018;19(11):3533.
22. Omar A, Kalra RS, Putri J, Elwakeel A, Kaul SC, Wadhwa R. Soyasapogenol-A targets CARF and results in suppression of tumor growth and metastasis in p53 compromised cancer cells. Sci Rep. 2020;10(1).
23. Weaver BA. How Taxol/paclitaxel kills cancer cells. Mol Biol Cell. 2014;25(18):2677-2681.
24. Aziz DZ, Hadi MA, Al-Kelaby KKA, Abdullah ZA, Hamza A, Altaee AA, et al. Cytotoxic and Antioxidant Activity of Linseeds Against Rhabdomyosarcoma Cell Line. Advancements in Life Sciences. 2023;10:67.
25. Khalida Abbas Al K, Qabas Neamah Hadi Al H, Ghaith Kadhim Al A. Sero-prevalence of Hepatitis C virus infection in patients undergoing haemodialysis in Al-Najaf Province. J Pak Med Assoc. 2023;73(9):S165-S167.
26. Sahayam J SA, M K, K V. Pattern of Adverse Drug Reactions of Anticancer Drugs Used in Patients with Non Hodgkin's Lymphoma in A Tertiary Care Hospital. IOSR Journal of Dental and Medical Sciences. 2016;15(08):104-108.
27. Coumarin Derivatives Containing Sulfonamide and Dithioacetal Moieties: Design, Synthesis, Antiviral Activity, and Mechanism. American Chemical Society (ACS).
28. Usman MS, Hussein MZ, Fakurazi S, Ahmad Saad FF. Gadolinium-based layered double hydroxide and graphene oxide nano-carriers for magnetic resonance imaging and drug delivery. Chem Cent J. 2017;11(1).
29. Farrell CL, Rex KL, Chen JN, Bready JV, DiPalma CR, Kaufman SA, et al. The effects of keratinocyte growth factor in preclinical models of mucositis. Cell Prolif. 2002;35(s1):78-85.
30. Galdino FMP, Andrade MER, Barros PAVd, Generoso SdV, Alvarez-Leite JI, Almeida-Leite CMd, et al. Pretreatment and treatment with fructo-oligosaccharides attenuate intestinal mucositis induced by 5-FU in mice. J Funct Foods. 2018;49:485-492.
31. Thorn CF, Oshiro C, Marsh S, Hernandez-Boussard T, McLeod H, Klein TE, et al. Doxorubicin pathways. Pharmacogenet Genomics. 2011;21(7):440-446.
32. Cytotoxicity of Magnesium Oxide-Zinc Oxide-Titanium Nanocomposite ($MgZnTiO_4$) on LS 174T Colorectal Adenocarcinoma Cell Line. International Journal of Pharmaceutical Research. 2019;11(02).
33. Ghasemi M, Turnbull T, Sebastian S, Kempson I. The MTT Assay: Utility, Limitations, Pitfalls, and Interpretation in Bulk and Single-Cell Analysis. Int J Mol Sci. 2021;22(23):12827.
34. Anand U, Dey A, Chandel AKS, Sanyal R, Mishra A, Pandey DK, et al. Cancer chemotherapy and beyond: Current status, drug candidates, associated risks and progress in targeted therapeutics. Genes & Diseases. 2023;10(4):1367-1401.
35. Krishnamoorthy K, Moon JY, Hyun HB, Cho SK, Kim S-J. Mechanistic investigation on the toxicity of MgO nanoparticles toward cancer cells. J Mater Chem. 2012;22(47):24610.
36. Varghese E, Samuel SM, Sadiq Z, Kubatka P, Liskova A, Benacka J, et al. Anti-Cancer Agents in Proliferation and Cell Death: The Calcium Connection. Int J Mol Sci. 2019;20(12):3017.